Available online at www.sciencedirect.com
SCIENCE DIRECT
Journal of Sound and Vibration 296 (2006) 1068–1078
JOURNAL OF SOUND AND VIBRATION
www.elsevier.com/locate/jsvi

Short Communication

Bifurcations and chaos in a forced cantilever system with impacts

Wang Lin*, Ni Qiao, Huang Yuying

Department of Mechanics, Huazhong University of Science and Technology, Wuhan 430074, People's Republic of China

Received 11 July 2005; received in revised form 1 March 2006; accepted 16 March 2006
Available online 5 May 2006

Abstract

The nonlinear dynamics of a cantilever system excited by a periodic force and taking into account the combined effects of impacts and nonlinear term due to the beam deflection is studied. Precise approximations of the beam deflection and consequently the overall stiffness are introduced to formulate the equation of motion for the cantilever system. Two impact models are investigated in this communication, respectively. One is a one-sided impact model, and the other is a both-sided impact model. Based on carefully numerical simulations, bifurcations and the possible chaotic motions for these two models are represented to show the combined effects of nonlinearities on the dynamics of these two models.

Keywords: Cantilever; Bifurcation; Chaos; Impact

1. Introduction

In recent decades, much attention has been given to the nonlinear dynamics of impact oscillators. In the impact oscillators, the systems with clearances between springs and mass were always considered by many investigators. And various modeling of dynamical systems have been developed with various types of clearances. Notable contributions were made by Peterka and Vacik [1], Wiercigroch [2], Peterka [3], Danca and Codreanu [4], Wiercigroch and Sin [5] and Shaw and Holmes [6]. From these and several other studies, it is clear that the main nonlinearities in such dynamical systems are caused by the discontinuities related to the clearances. Moreover, variants thereof are capable of displaying an extremely rich and variegated dynamical behaviour. Thus, the impact systems are fast becoming important paradigms in dynamics.

If, however, the mass is a part of a larger system, the nonlinearities in the system may contain the nonlinearities due to clearances and other ones. In this case, significant errors can be induced when investigating the dynamical behaviour, both quantitatively and qualitatively, by neglecting even small nonlinearities. This is particularly true in the system contains those nonlinearities such as clearances or boundary conditions, known to be conducive of rich dynamical responses. It is well known that a common beam can produce nonlinearity due to its own deflection. Hence, by considering the clearances between the

*Corresponding author. Tel.: +86 27 87543438; fax: +86 27 87543138.
E-mail address: wanglinfliping@sohu.com (W. Lin).

0022-460X/$ - see front matter © 2006 Elsevier Ltd. All rights reserved.
doi:10.1016/j.jsv.2006.03.015

mass and springs, if the mass is attached to a beam at the tip end, complex nonlinearities exist in such a system during its vibrating. To the authors' best knowledge, very few researches have been done on the combined effects of clearance-nonlinearity and other nonlinearities in such a large beam system. Maybe the first important work in this area was done by Emans et al. [7]. In their study, a common cantilever beam attached with a mass at the tip was considered. The commonly encountered physical system is with two different nonlinearities, the first coming from intermittent contact with another body, the second from the reaction of a cantilever beam system due to its deflection.

The aims of this communication are twofold. Firstly, we will extend the work by Emans et al. [7]. In Ref. [7], the impact model is a one-sided spring with a clearance; a comparison between the piecewise nonlinear and piecewise linear system responses was made to show the effect due to beam deflection. However, only a specific set of system parameters were chosen for calculations in their study. Thus, the effects of each system parameters on the dynamics of the one-sided system are not revealed yet. In this paper, bifurcation diagrams of several key system parameters will be constructed and typical motions of the system shown. Secondly we investigate numerically, for the first time, a cantilever system with both-sided springs in which the cumulative effect of two nonlinearities are considered. It will be shown that rich dynamics occurs in these two impact models. The corresponding comparison is made between these two cases and the differences found are briefly discussed and some possible explanations put forward.

2. Background theory

Consider a simple cantilever beam system as shown in Fig. 1. The system comprises of two leaf springs and a mass M. The length of the beam is L and bending stiffness EI. Hence, the boundary conditions can prevent rotation of the mass. Moreover, the mass is excited by a force $F = F_0 \cos(\omega t)$.

This may be a common beam arrangement, used as a typical structural element in buildings, with the mass representing a floor. However, the beam will react on the mass when the mass is vibrating. The reaction can be considered as a storing force. Thus, to fully study the dynamics and behaviour of such an arrangement it is needed to develop accurate formulae for the beam stiffness. Recently, the study [7] has given precise approximations of the beam deflection and the overall stiffness.

According to Ref. [7], the reaction expression for a single beam can be constituted as follows:

$$R = 12\frac{EI}{L^3}x + \frac{432}{35}\frac{EI}{L^5}x^3 \tag{1}$$

in which x is the deflection of the beam at $s = L$.

Hence, for a simple one degree-of-freedom system shown in Fig. 1, the dynamics of this system can be described by the following differential equation:

$$M\ddot{x} + c\dot{x} + 12\frac{EI}{L^3}x + \frac{432}{35}\frac{EI}{L^5}x = F_0 \cos(\omega t), \tag{2}$$

where c is the internal damping coefficient, F_0 and ω the forcing amplitude and frequency of an external force.

One can see that Eq. (2) is similar to the Duffing system, which is well known to give rich nonlinear dynamical behaviour such as coexistence of attractors and chaotic vibrations. However, as demonstrated in Ref. [7], chaos was found in the system described in Eq. (2) with physically unrealistic parameters, and no

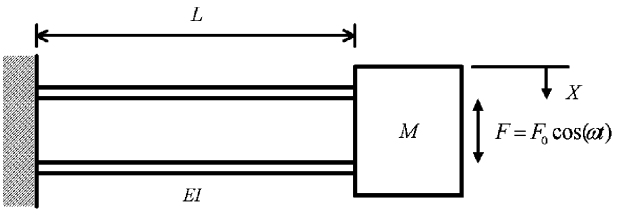

Fig. 1. A cantilever beam system with no impact.

chaos was detected with physically realistic parameters. Thus, only periodic responses were found readily for the physically realistic parameters.

3. The forced cantilever beam system with one-sided impact

In this section, a one-sided impact system shown in Fig. 2 will be investigated in detail. Of course, this system has been preliminarily studied by Emans et al. [7]. However, as mentioned above, only a specific set of system parameters were chosen for calculations in their study. The effects of each key system parameters on the dynamics of the one-sided system are not revealed yet.

The nonlinear equation of motion for the beam system, with nonlinear approximation for beam reaction is as follows:

$$M\ddot{x} + c\dot{x} + 12\frac{EI}{L^3}x + \frac{432}{35}\frac{EI}{L^5}x + KH(x)(x - e_0) = F_0\cos(\omega t), \tag{3}$$

where K is the stiffness of the spring; $H(x)$ is the Heaviside step function, which has the following form:

$$H(x) = \begin{cases} 0; & x < e_0, \\ 1; & x \geqslant e_0. \end{cases} \tag{4}$$

For purposes of numerical simulations, Eq. (3) is reduced to its first-order form,

$$\begin{aligned} \dot{y} &= z, \\ z &= \beta\cos(\Omega\tau) - 2\xi z - \tfrac{36}{35}y^3 - kH(y)(y - \hat{e}_0). \end{aligned} \tag{5}$$

Obviously, Eq. (5) is a nondimensional equation, and some dimensionless quantities are defined as

$$y = \frac{x}{L}, \quad \tau - \omega_0 t, \quad \xi = \frac{c}{2\omega_0 M}, \quad \beta = \frac{F_0}{\omega_0^2 ML}, \quad \Omega = \frac{\omega}{\omega_0}, k = \frac{KL^3}{12EI}, \quad \hat{e}_0 = \frac{e_0}{L}, \quad \omega_0 = \sqrt{\frac{12EI}{ML^3}}. \tag{6}$$

Solutions of Eq. (5) were obtained by using a fourth order Runge-Kutta integration algorithm, with a step size of 0.01; the initial conditions employed were $y(0) = 0.001, \dot{y}(0) = 0$. The accuracy of this integration algorithm is very good provided that the integration step size is not too large. In fact, in this study, even the step size is chosen to be a sufficiently small one (e.g. 0.001), the corresponding numerical results have shown to be very close to those obtained with a step size of 0.01. It is noted that, a very similar dynamical system so-called "pipe conveying fluid" also has cumulative nonlinearities due to geometry and impacts (see Ref. [8]). In the study of Ref. [8], the first-order equations of the pipe model were solved by the fourth order Runge-Kutta algorithm with an integration step size of 0.005. Numerical results for the nonlinear pipe with impacts have shown good agreement with those observed in experiments. Moreover, the pipe system developed in Ref. [8] was essentially modeled as a beam model. Hence, the fourth order Runge-Kutta algorithm with a reasonable step size can capture the main dynamical behaviour of the beam system with cumulative nonlinearities.

Based on the integration algorithm mentioned above, numerical calculations have produced the bifurcation diagram of Fig. 3, as the forcing amplitude (β) is varied in the range $0.1 \leqslant \beta \leqslant 0.5$, and the values of other

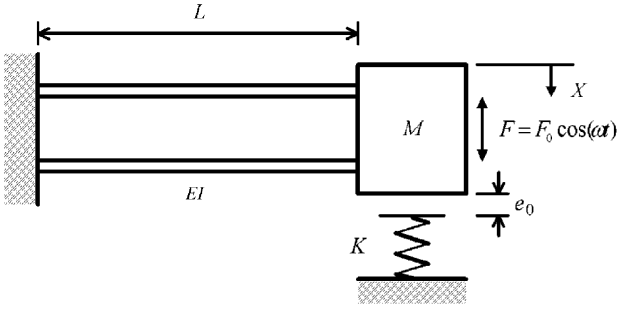

Fig. 2. A cantilever beam system with one-sided impact.

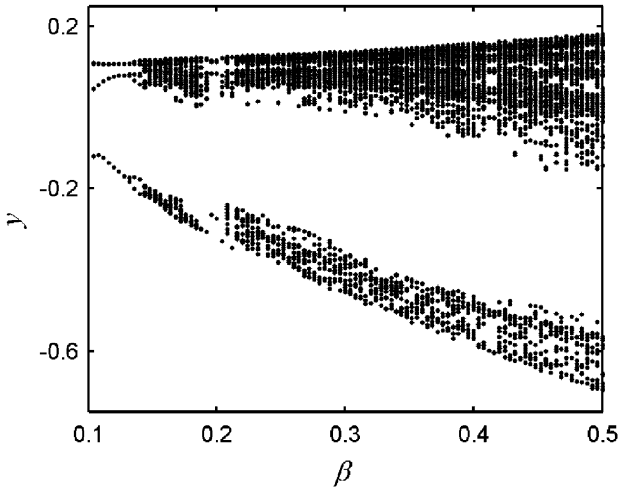

Fig. 3. Bifurcation diagram: the displacement as a function of the forcing amplitude, and $\xi = 0.02$, $\Omega = 0.2$, $k = 25$, $\hat{e}_0 = 0.1$.

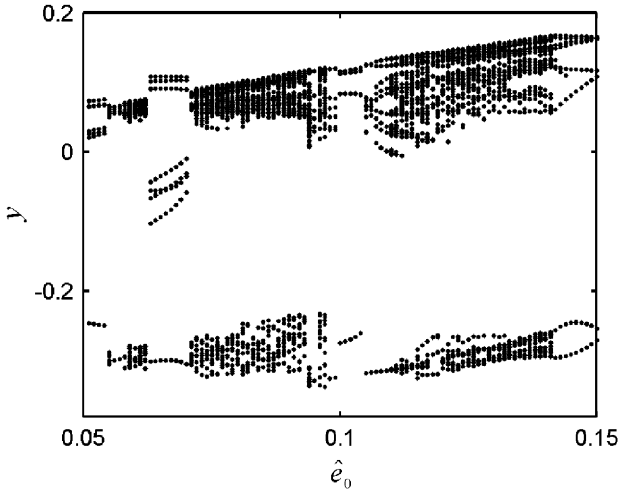

Fig. 4. Bifurcation diagram: the displacement as a function of the clearance, and $\xi = 0.02$, $\Omega = 0.2$, $k = 25$, $\beta = 0.2$.

parameters are all fixed. Similarly, Figs. 4–7 represent the bifurcation diagrams as several other key system parameters are chosen to be varied. In these figures the y plotted in the ordinate is the amplitude of the displacement of the mass. In the calculations, the transient solutions were discarded. Hence, whenever the velocity of the mass, $\dot{y}$, was zero, the displacement of the mass was recorded—thus producing both positive and negative values, as shown in Figs. 3–7.

From Fig. 3, we can see that the amplitude of the motion is increasing with the increasing forcing amplitude. When forcing amplitude is approximately less than 0.13, the mass tends to undergo periodic motions. However, for $\beta \geqslant 0.13$, chaotic motions may occur in a large range of β; and the chaotic vibrations of the mass are narrow-band ones, as can be seen in Fig. 3. As the mass is not restrained in the negative direction, big amplitudes occurs with a large β; and the negative amplitude of the mass is much larger than the positive one. Moreover, there are relatively sub regions of periodic motions embedded with the chaotic region; e.g. for $0.19 \leqslant \beta \leqslant 0.2$ there is what appears to be a period-3 region. Similarly, in the parameter spaces of several other key parameters (i.e., e_0, k, and Ω), the system is also capable of displaying rich dynamical behaviour. In the parameter space of e_0, chaotic and periodic motions alternately occur; and discontinuities (jumps) arise at some values of e_0, the nature of which is not understood (see Fig. 4). Further, discontinuities can also be found

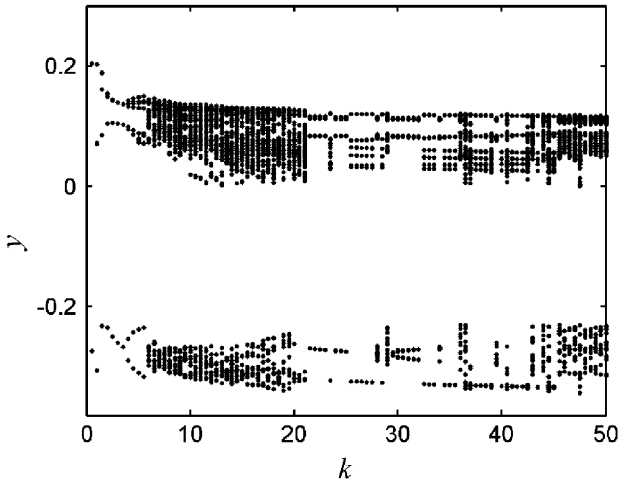

Fig. 5. Bifurcation diagram: the displacement as a function of the stiffness of the spring, and $\xi = 0.02$, $\Omega = 0.2$, $\hat{e}_0 = 0.1$, $\beta = 0.2$.

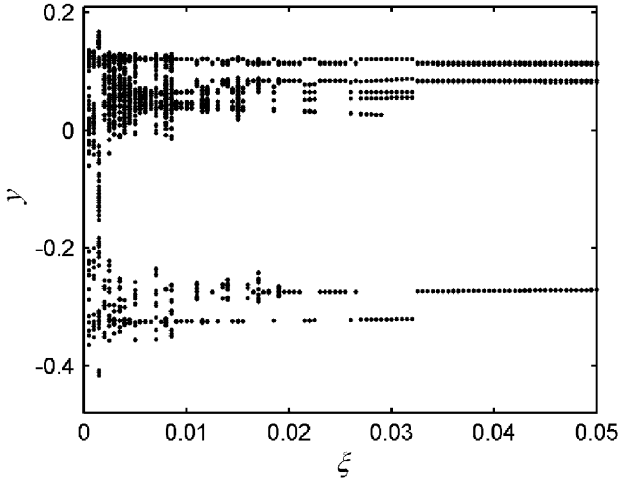

Fig. 6. Bifurcation diagram: the displacement as a function of the forcing amplitude, and $\Omega = 0.2$, $k = 25$, $\hat{e}_0 = 0.1$, $\beta = 0.2$.

in Fig. 5, as the spring stiffness is varied. In Fig. 6, the varied parameter is ξ. When ξ is small ($0 \leqslant \xi \leqslant 0.08$), the bifurcation diagram shows the vibrations of the mass are in the chaotic regime; however, when ξ is much larger ($\xi > 0.08$), the system always behaves periodic motions. In the parameter space of Ω, chaotic and periodic motions alternately occur when Ω is varied in the range of $0.3 \leqslant \Omega \leqslant 0.48$ as opposed to only periodic ones can be detected when Ω is varied in the range of $0.7 > \Omega > 0.48$.

It is instructive to look at phase-plane portraits associated with various values of e_0 (or other system parameters), corresponding to different dynamical behaviour as discussed in the foregoing. The results are shown in Fig. 8. In Figs. 8 (b) and (e), the system behaves chaotic motions. The remaining parts of Fig. 8, from which the initial transients have been omitted for clarity, show various periodic motions. Thus, one can see that the cantilever system can display rich dynamical behaviour. It should be remarked that, the dynamics is related to the combined nonlinearities of the system. The nonlinearities in this one-sided impact system comprise of two parts, as mentioned in the foregoing.

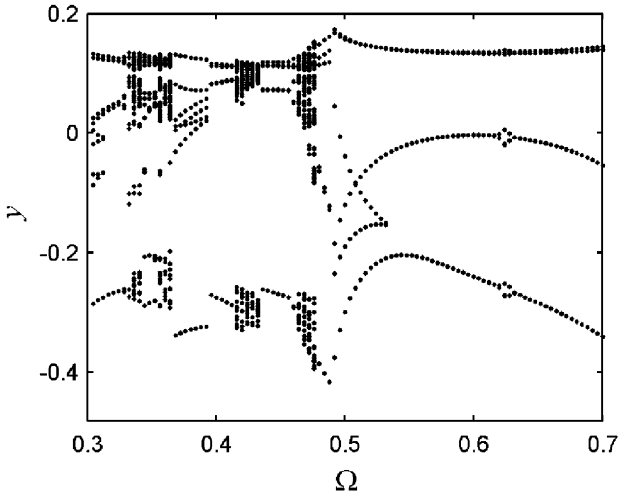

Fig. 7. Bifurcation diagram: the displacement as a function of the forcing frequency, and $\xi = 0.02$, $k = 25$, $\hat{e}_0 = 0.1$, $\beta = 0.2$.

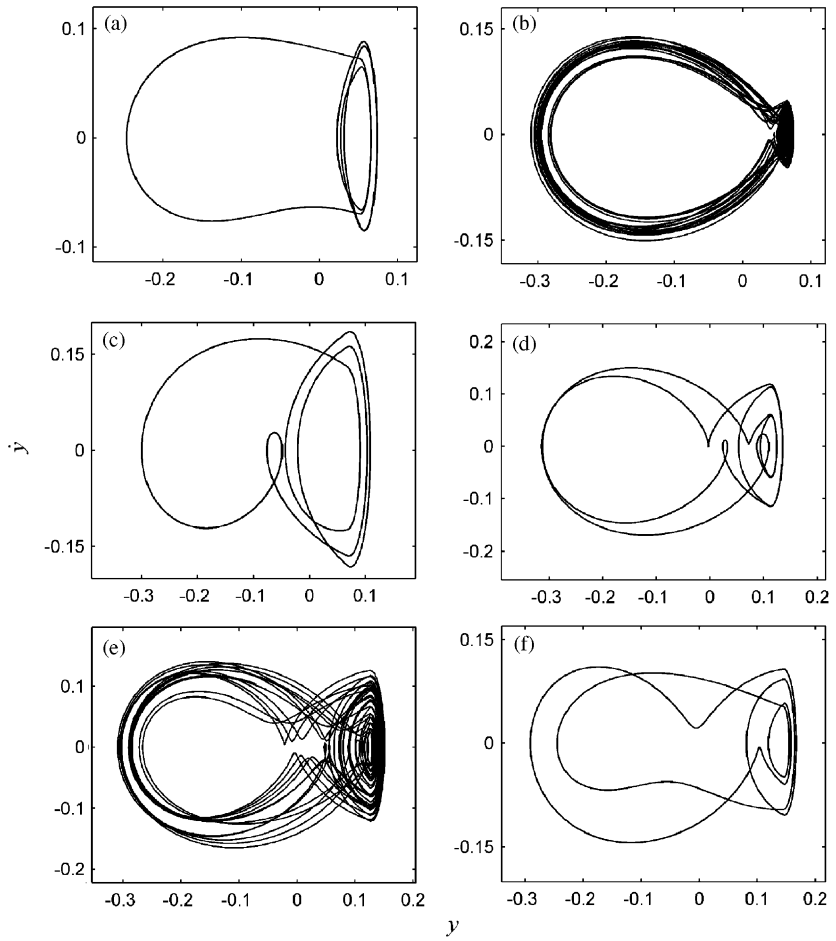

Fig. 8. Phase portraits for $\xi = 0.02$, $\Omega = 0.2$, $k = 25$, $\beta = 0.2$, and different values of $\hat{e}_0$: (a) $\hat{e}_0 = 0.052$, (b) $\hat{e}_0 = 0.06$, (c) $\hat{e}_0 = 0.068$, (d) $\hat{e}_0 = 0.11$, (e) $\hat{e}_0 = 0.125$, and (f) $\hat{e}_0 = 0.145$.

4. The forced cantilever beam system with both-sided impacts

In this section a modified cantilever system shown in Fig. 9 is further investigated. It can be seen that this cantilever system has both-sided impacts. The stiffness of two springs is denoted as K_1 and K_2, respectively. The clearances between the mass and the springs are e_1 and e_2. In what follows, e_1 and e_2 (or K_1 and K_2) may be different from each other in the calculations.

Similarly, by considering the effects of both-sided impacts, the nonlinear equation of the cantilever system may be written as:

$$M\ddot{x} + c\dot{x} + 12\frac{EI}{L^3}x + \frac{432}{35}\frac{EI}{L^5}x + G(x) = F_0\cos(\omega t) \tag{7}$$

in which $G(x)$ denotes a piecewise function

$$G(x) = \begin{cases} K_1(x - e_1) & x > e_1, \\ 0; & -e_2 \leqslant x \leqslant e_1, \\ K_2(x + e_2); & x < -e_2. \end{cases} \tag{8}$$

Eq. (7) can be further transformed into its first-order form

$$\begin{aligned} \dot{y} &= z, \\ z &= \beta\cos(\Omega\tau) - 2\xi z - \tfrac{36}{35}y^3 - g(y), \end{aligned} \tag{9}$$

where

$$\begin{gathered} y = \tfrac{x}{L}, \quad \tau = \omega_0 t, \quad \xi = \tfrac{c}{2\omega_0 M}, \quad \beta = \tfrac{F_0}{\omega_0^2 ML}, \quad \Omega = \tfrac{\omega}{\omega_0}, \quad k_1 = \tfrac{K_1 L^3}{12EI}, \\ k_2 = \tfrac{K_2 L^3}{12EI} \quad \hat{e}_1 = \tfrac{e_1}{L}, \quad \hat{e}_2 = \tfrac{e_2}{L}, \quad \omega_0 = \sqrt{\tfrac{12EI}{ML^3}}, \end{gathered} \tag{10}$$

and

$$g(y) = \begin{cases} k_1(y - \hat{e}_1); & x > \hat{e}_1, \\ 0; & -\hat{e}_2 \leqslant x \leqslant \hat{e}_1, \\ k_2(y + \hat{e}_2); & x < -\hat{e}_2. \end{cases} \tag{11}$$

Similarly as before, solutions of Eq. (9) were obtained by using a fourth-order Runge-kutta method, with the same step size and initial conditions employed in the foregoing. Figs. (10–14) show the bifurcation diagrams for the displacement of the mass, as several key system parameters are varied, respectively. In Fig. 10, the variable parameter is the dimensionless forcing amplitude β. The bifurcation diagram shows that the chaotic motion is a wide-band one. If, however, the both-sided impacts are symmetric (i.e. $e_1 = e_2$ and $K_1 = K_2$), the displacement (y) plotted in the ordinate is generally symmetric, as can be seen in Figs. 10, 13 and

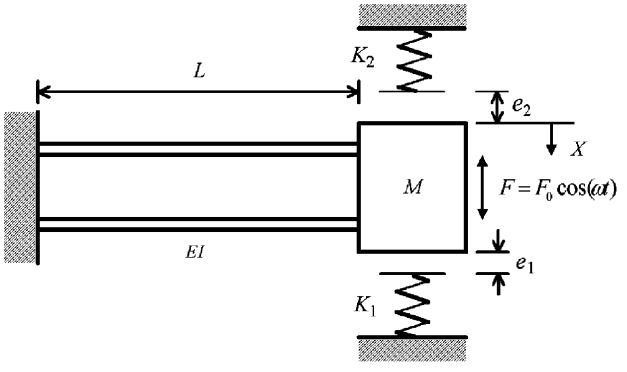

Fig. 9. A cantilever beam system with both-sided impacts.

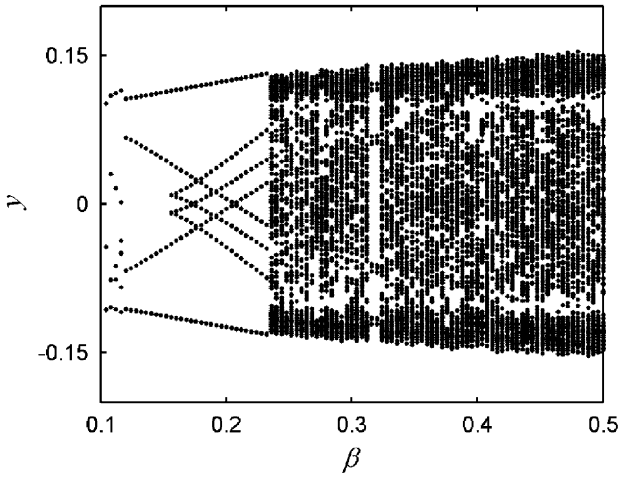

Fig. 10. Bifurcation diagram: the displacement as a function of the forcing amplitude, and $\xi = 0.02$, $\Omega = 0.4$, $k_1 = 50$, $k_2 = 50$, $\hat{e}_2 = 0.1$, $\hat{e}_2 = 0.1$.

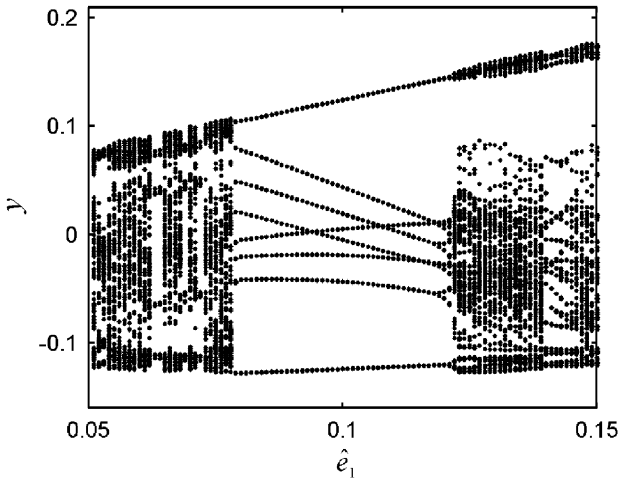

Fig. 11. Bifurcation diagram: the displacement as a function of $\hat{e}_1$, and $\xi = 0.02$, $\Omega = 0.4$, $k_1 = 50$, $k_2 = 50$, $\hat{e}_2 = 0.1$, $\beta = 0.2$.

14. This may be different from that of the one-sided impact system. It should be also noted that, for a system defined by $\Omega = 0.4$, $k_1 = 50$, $k_2 = 50$, $\hat{e}_2 = 0.1$, $\hat{e}_2 = 0.1$, $\beta = 0.2$, only period-5 motion can be detected as ξ is varied in the range $0 \leqslant \xi \leqslant 0.05$.

Indeed, if the stiffness of the two springs are reasonable large, the both-sided impacts evidently "kill" the big amplitudes appeared in the one-sided impact system, as can be clearly seen in Figs. (10–14). However, the amplitude may become big if one (or two) of the stiffness is extremely small (e.g. $k_2 = 1$) with the same other parameter values chosen as before.

Fig. 15 represents phase-plane portraits for several typical motions for different values of Ω. Various periodic and chaotic motions can be clearly seen. From a physical point of view, the dynamics of the mechanism is related to the interaction of two nonlinearities, as discussed in the foregoing.

5. Conclusion

In this short communication, the nonlinear dynamics of a common cantilever beam system, with impacts and excited by a periodic force, was explored numerically. However, more broadly, this is a multidimensional

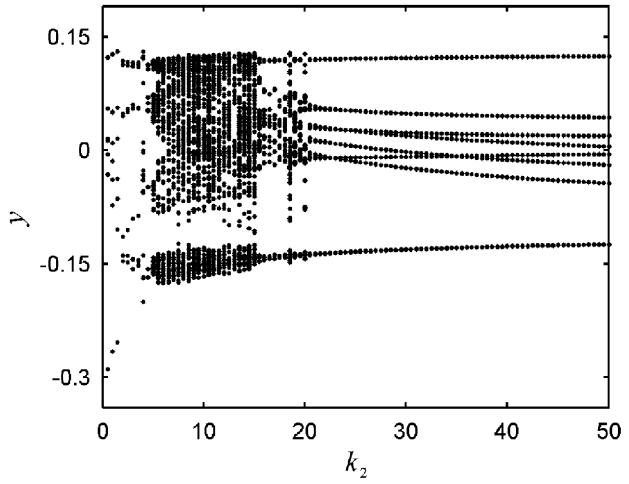

Fig. 12. Bifurcation diagram: the displacement as a function of k_2, and $\xi = 0.02$, $\Omega = 0.4$, $k_1 = 50$, $\hat{e}_2 = 0.1$, $\hat{e}_2 = 0.1$, $\beta = 0.2$.

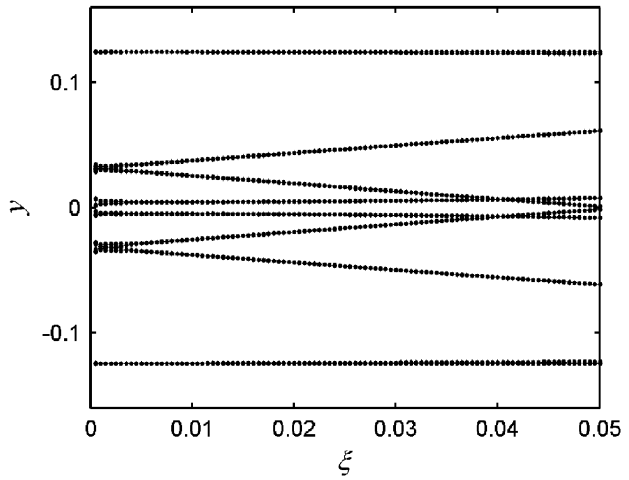

Fig. 13. Bifurcation diagram: the displacement as a function of ξ, and $\Omega = 0.4$, $k_1 = 50$, $k_2 = 50$, $\hat{e}_2 = 0.1$, $\hat{e}_2 = 0.1$, $\beta = 0.2$.

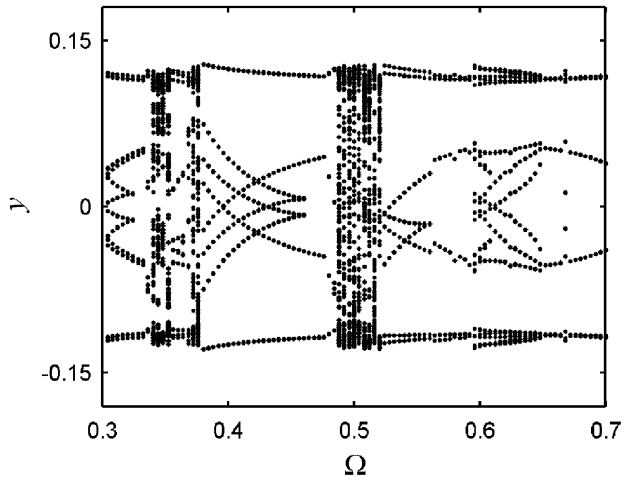

Fig. 14. Bifurcation diagram: the displacement as a function of Ω, and $\xi = 0.02$, $k_1 = 50$, $k_2 = 50$, $\hat{e}_2 = 0.1$, $\hat{e}_2 = 0.1$, $\beta = 0.2$.

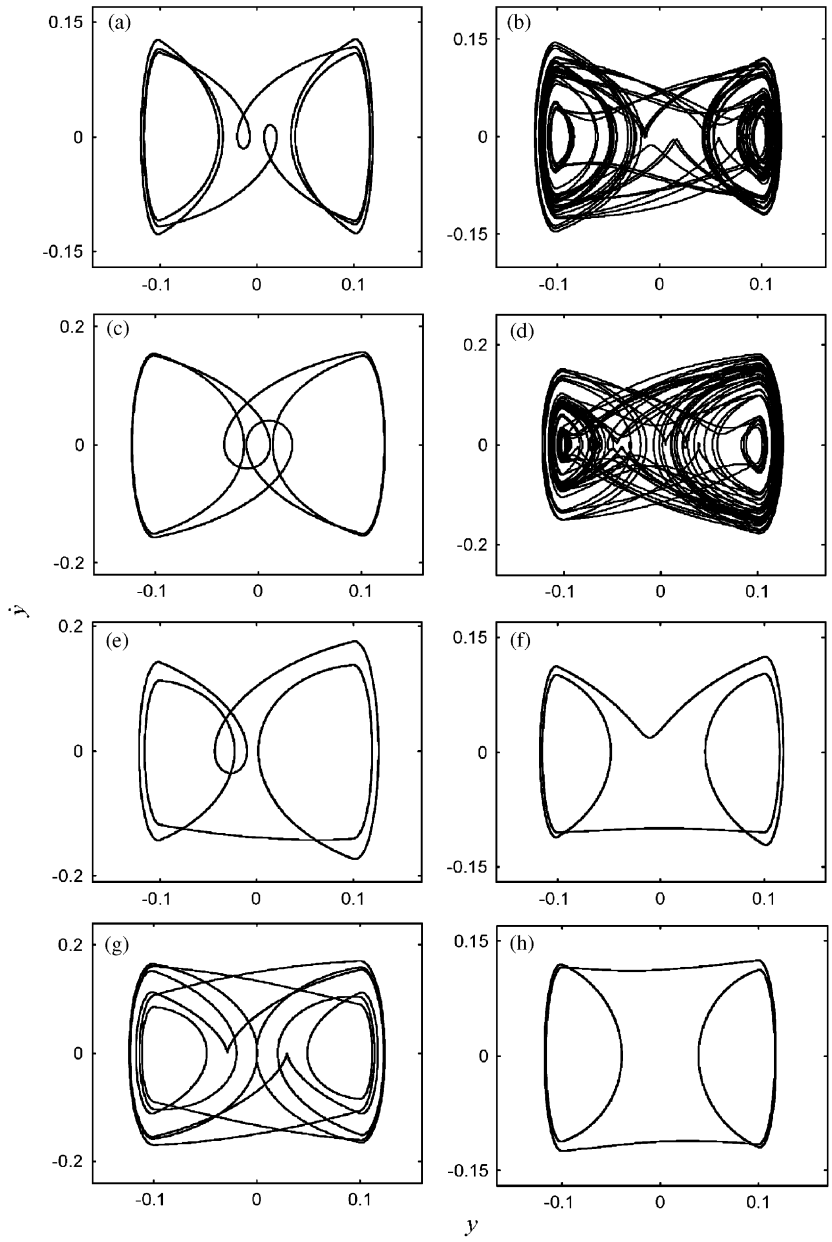

Fig. 15. Phase portraits for $\xi = 0.02$, $k_1 = 50$, $k_2 = 50$, $\hat{e}_2 = 0.1$, $\hat{e}_2 = 0.1$, $\beta = 0.2$, and different values of Ω: (a) $\Omega = 0.31$, (b) $\Omega = 0.35$, (c) $\Omega = 0.41$, (d) $\Omega = 0.5$, (e) $\Omega = 0.53$, (f) $\Omega = 0.58$, (g) $\Omega = 0.61$, and (h) $\Omega = 0.7$.

investigation of the effects of (i) the nonlinearity of the type associated with the beam deflection, (ii) the impact models with springs and clearances.

The behaviour was analysed for two impact models. For the one-sided impact model, various periodic motions were found as well as existence of chaotic motions. Bifurcation diagrams and phase-plane portraits were constructed to show the rich dynamical behaviour of the one-sided system. Then another both-sided impact model was further investigated. The corresponding comparison is made between these two models and the differences found are briefly discussed. It is also found that the magnitudes of the vibrating displacement and velocity are equal, both for the one-sided and both-sided impact models. Hence, these two impact models represent low velocity impacts.

However, for the beam arrangement developed in this paper, experiment would be done to clarify its dynamics. To advance in this direction, an experimental study has been initiated, which should help grasp the truth closer.

References

[1] F. Peterka, J. Vacik, Transition to chaotic motion in mechanical systems with impacts, *Journal of Sound and Vibration* 154 (1) (1992) 95–115.
[2] M. Wiercigroch, Bifurcation-analysis of harmonically excited linear oscillator with clearance, *Chaos, Solitons & Fractals* 4 (2) (1994) 297–303.
[3] F. Peterka, Bifurcations and transition phenomena in an impact oscillator, *Chaos, Solitons & Fractals* 7 (10) (1996) 1635–1647.
[4] M.F. Danca, S. Codreanu, On a possible approximation of discontinuous dynamical systems, *Chaos, Solitons & Fractals* 13 (4) (2002) 681–691.
[5] M. Wiercigroch, V.W.T. Sin, Experimental study of a symmetrical piecewise base-excited oscillator, *Journal of Applied Mechanics-Transition of the ASME* 65 (3) (1998) 657–663.
[6] S.W. Shaw, P.J. Holmes, A periodically forced piecewise linear-oscillator, *Journal of Sound and Vibration* 90 (1) (1983) 129–155.
[7] J. Emans, M. Wiercigroch, A.M. Krivtsov, Cumulative effect of structural nonlinearities: chaotic dynamics of cantilever beam system with impacts, *Chaos, Solitons & Fractals* 23 (2005) 1661–1670.
[8] M.P. Paidoussis, C. Semler, Nonlinear and Chaotic Oscillations of a constrained cantilevered pipe conveying fluid: a full nonlinear analysis, *Nonlinear Dynamics* 4 (1993) 655–670.